International Journal of Energy and Environmental Science
2023; 8(5): 100-106
http://www.sciencepublishinggroup.com/j/ijees
doi: 10.11648/j.ijees.20230805.12
ISSN: 2578-9538 (Print); ISSN: 2578-9546 (Online)

Photoelectrocatalytic Degradation of Chlorpyrifos Wastewater Paired with Biogas SOFC Based on $PrBaMn_2O_{5+\delta}$ Electrodes

Doudou Gu[1], Guan Zhang[1], Jing Zou[2, *]

[1]School of Civil and Environmental Engineering, Harbin Institute of Technology, Shenzhen, P. R. China

[2]General Education Division, The Chinese University of Hong Kong, Shenzhen, P. R. China

Email address:

zoujing@cuhk.edu.cn (Jing Zou)

[*]Corresponding author

To cite this article:

Doudou Gu, Guan Zhang, Jing Zou. Photoelectrocatalytic Degradation of Chlorpyrifos Wastewater Paired with Biogas SOFC Based on $PrBaMn_2O_{5+\delta}$ Electrodes. *International Journal of Energy and Environmental Science*. Vol. 8, No. 5, 2023, pp. 100-106.
doi: 10.11648/j.ijees.20230805.12

Received: September 5, 2023; **Accepted**: September 28, 2023; **Published**: October 14, 2023

Abstract: In recent years, photocatalytic oxidation (PEC) technology has been widely studied in the field of water pollution remediation as an effective way to accelerate the degradation rate of organic matter. However, the external electric field applied by commonly used PEC wastewater treatment tanks is mostly provided by external equipment, therefore the pollution reduction process is accompanied by inevitable additional energy consumption. Aimed to reduce energy consumption and carbon emission, we designed a PEC tank which gets the extra bias voltage input from a biogas solid oxide fuel cell (SOFC) based on $PrBaMn_2O_{5+\delta}$ electrodes. The $PrBaMn_2O_{5+\delta}$ (PBMO) double perovskite powder has mainly tetragonal phase in both reduced and oxidized atmosphere. The polarization resistances of the PBMO electrodes with PBMO|SDC functional layers were 0.08 and 0.78 $\Omega \cdot cm^2$ in air and simulated biogas respectively. Using simulated biogas (70% CH_4 and 30% CO_2) with 3% water vapor as the fuel and ambient air as the oxidant, the SOFC power density can achieve 325.5 and 234.8 $mW \cdot cm^{-2}$ at 700 and 650°C, respectively. Using MoS_2/Ti as photoanode for the PEC tank, with applied bias of 0.5 V in 0.02 M Na_2SO_3 electrolyte, and with pH=3, the degradation rate of chlorpyrifos (CPF) in PEC tank can achieve 99.7% after 4 hours.

Keywords: Photoelectrocatalytic, Biogas, SOFC

1. Introduction

The carbon emissions of the sewage treatment industry account for about 1% of the total emissions of society, and it accounts for the largest proportion in the environmental protection industry. [1] Sewage treatment requires a large amount of fuel and chemicals, indirectly emitting a large amount of greenhouse gases. The treatment process itself also directly emits greenhouse gases. During the sewage treatment process, biogas is discharged, which contains CO_2, CH_4, and other components such as N_2O. These waste gases are often directly discharged into the atmosphere after simple desulfurization and deodorization treatments, and a small amount of them are burned by heat engines to generate pollutants such as nitrogen oxides, which increases air pollution and greenhouse gas emissions, while also causing resource waste.

In addition, although the energy consumption of the sewage treatment industry is not as high as that of industries such as power generation, steel, and chemical engineering, the proportion of total energy consumption is not small, and it is also a major energy consumer. From the perspective of energy conversion, the essence of traditional sewage treatment mode is to exchange energy consumption for water quality. In order to reduce water pollution, we need to use a large amount of electricity. [2]

Photocatalysis refers to the direct use of light energy by various semiconductor materials at room temperature to completely mineralize and remove various organic pollutants, becoming an ideal environmental pollution control technology. When the energy is equal to or greater than the band gap the of semiconductor material, the photoelectrons are excited to the

conduction band, and photo-generated holes are generated in the valence band. Photo-generated holes can capture electrons in organic matter or solution on the surface of semiconductor particles, so that substances that do not absorb light are activated and oxidized. Therefore, they have strong oxidation capacity. Organic matter is oxidized directly or indirectly, and eventually degraded into simple inorganic compound substances such as CO_2 and H_2O. Compared with photocatalysis, photoelectrocatalytic (PEC) oxidation technology needs an extra bias voltage, which efficiently improves the separation of photoelectrons and holes, improves quantum efficiency, and thus accelerates the degradation rate of organic pollutants in wastewater. [3]

However, the external electric field applied by commonly used PEC wastewater treatment tanks is mostly provided by external equipment such as electrochemical workstations, and the pollution reduction process is accompanied by inevitable additional energy consumption. [4] The large amount of carbon containing waste gas generated by landfills and sewage treatment plants that can be used for power generation has not been recycled as a resource, which cannot effectively achieve the synergistic goal of reducing pollution, energy conservation and low carbon emission.

As a device that can directly convert chemical energy into electrical energy, solid oxide fuel cells (SOFCs) have the advantages of high power generation efficiency, low pollution emissions, and a wide range of fuel applications. The direct use of biogas and other fuels for power generation is one of the important development directions of SOFCs, because the methane in biogas can be converted into hydrogen rich synthesis gas on the anode side of the SOFCs with the help of CO_2, which generates electricity through high-temperature catalytic chemical reactions on the anode. [5, 6]

However, when using hydrocarbon-rich gases such as methane or biogas as fuel, because Ni has a catalytic effect on carbon deposition, it will cause carbon deposition and cause nickel to lose its catalytic activity. Researchers have begun various attempts to solve the problems that anodes pose when faced with carbon-based fuels. The attempts made can be divided into two categories. One is still based on the cermet (such as Ni/YSZ) system, modifying the cermet through doping, etc., or using other materials to replace Ni or YSZ; the other is the use of materials with different structures such as oxides with mixed ion/electronic conductivity properties. Among them, the oxides that can maintain stable structure and performance within a wide oxygen partial pressure and temperature range have received great attention. Representative materials include $La_{1-x}Sr_xCr_{1-y}M_yO_3$ (M=Mn, Fe, Co, Ni) [7, 8], Ce or transition metals such as Ni, Co, Cu, Cr and Fe doped (La, Sr) TiO_3 [9-11], $SrMg_{1-x}Mn_xMoO_6$, etc., these anode materials have improved to varying degrees in terms of resistance to carbon deposition and sulfur poisoning.

Chen et al. used GDC-impregnated $La_{0.75}Sr_{0.25}Cr_{0.5}Mn_{0.5}O_3$ as the anode to achieve CH_4 internal reforming on a LSM/YSZ cathode-supported battery. When H_2 is used as the fuel, the energy density of the prepared fuel cell is comparable to that of Ni/YSZ as the anode. However, when CH_4 is used as fuel, its energy density is lower than that of H_2 fuel. Moreover, the material behaves unstable when sulfur is contained in the fuel [12]. Huang et al. studied the reforming and sulfur resistance properties of double perovskite $Sr_2Mg_{1-x}Mn_xMoO_{6-\delta}$ on SOFC anodes. The CH_4 reforming effect and sulfur resistance of $Sr_2MgMoO_{6-\delta}$ material as anode are better than $(La_{0.75}Sr_{0.25})_{0.9}Cr_{0.5}Mn_{0.5}O_{3-\delta}$ [13, 14]. Liu et al. found that $BaZr_{0.1}Ce_{0.7}Y_{0.2-x}Yb_xO_{3-\delta}$ co-doped with Y and Yb has strong resistance to carbon deposition and sulfur poisoning. When the fuel is switched to contain 50 ppm hydrogen sulfide, its output power basically does not change and can operate continuously and stably in dry propane for more than 100 hours [15].

Due to the structural flexibility of double perovskite oxide materials, they are able to maintain the perovskite structure while forming a reducing phase. A typical representative is the A-site ordered layered double perovskite $PrBaMn_2O_{5+\delta}$ (PBMO) jointly reported by the research groups of Irvine and Kim [16]. PBMO is stable over a wide range of oxygen partial pressure and temperature and shows good catalytic activity for hydrocarbon oxidation reactions. In the joint report of the research groups of Ishihara and Kim [17], it was shown that when the operating temperature is 700°C and a bias voltage of 0.6V is given, the Ca-doped PBMO-$PrBa_{0.8}Ca_{0.2}Mn_2O_5$ can operate in a humidified environment. It remains stable in isooctane for 50 hours; and continues to remain stable in humidified propane for 150 hours, and outputs a current density of 0.2-0.3A/cm^2. Yifei Sun [18] et al. studied the catalytic activity of Mo-doped $Pr_{0.5}Ba_{0.5}MnO_{3-\delta}$ in H_2 and CH_4 atmospheres. The report pointed out that after Mo doping, Mo-$Pr_{0.5}Ba_{0.5}MnO_{3-\delta}$ has a specific $Pr_{0.5}Ba_{0.5}MnO_{3-\delta}$ has more oxygen holes, so its catalytic activity is also improved. According to the above reports, the stability of PBMO in different atmospheres and temperatures and its resistance to carbon deposition and sulfur poisoning make it a very attractive anode material.

Therefore, in order to reduce the total energy consumption and low greenhouse gas emission in traditional wastewater treatment facilities, we designed a PEC wastewater treatment tank paired with biogas SOFCs based on PBMO electrode, aimed to utilize the biogas discharged in traditional sewage treatment process or garbage landfill processes to generate electricity, and tried to make use of the SOFC generated electricity to degrade organic pollutants by PEC tanks.

2. Experimental

2.1. Design of the Photoelectrocatalytic Apparatus Powered by Biogas SOFC (s)

Figure 1 is the schematic diagram to show the design of the photoelectrocatalytic (PEC) wastewater treatment tank paired with biogas SOFC (s). During operation, when the photocatalysis anode receives a certain energy from the light source, the electrons will be activated from the valence band to the conduction band, producing electrons and holes, which have strong oxidizing and reducing properties respectively.

The photo-generated holes react with the solution to form active free radicals, which can break the chemical bond of organic pollutants to degrade them, and finally generate CO_2 and water. Biogas SOFC (s) convert the chemical energy contained in biogas (which is produced in the biological treatment process and sludge fermentation process) into electrical energy, providing bias voltage for the photocatalytic cell, thereby forming the PEC tank and effectively enhancing the separation of photoelectrons and holes. Wastewater containing organic pollutants is injected into the PEC tank, and the pollutants fully react with free radicals and other substances generated by semiconductor photoelectrodes. And the waste gas produced in the SOFC anode contains high-temperature water vapor, which can be re-used to provide heat to the biological treatment tank and sludge fermentation tank.

In the following experiments, the possibility to use this SOFC powered PEC system to degrade organic water pollutant was tested.

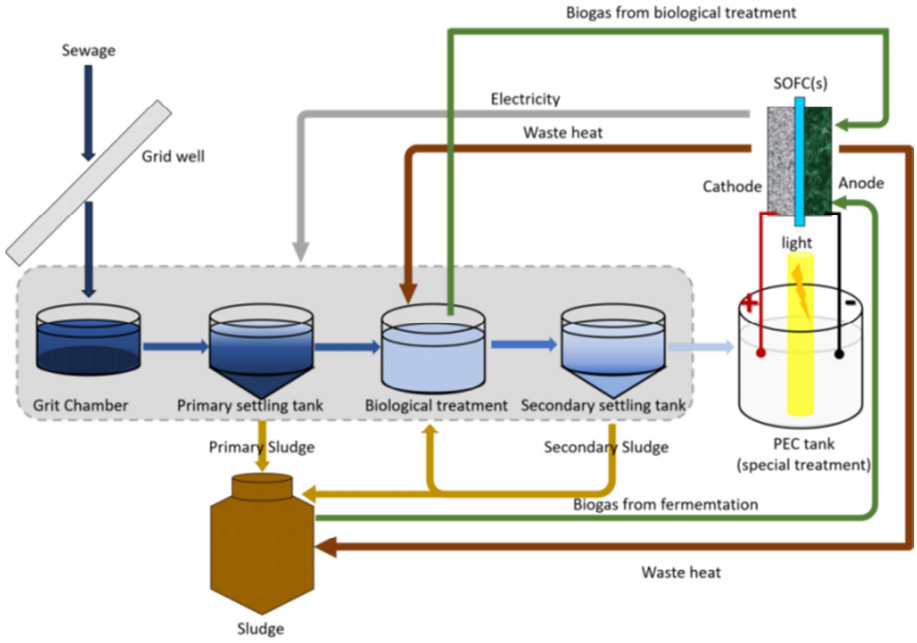

Figure 1. *Schematic diagram of the biogas SOFC (s) powered photoelectric catalytic (PEC) wastewater treatment tank.*

2.2. Material Preparation and Solid Oxide Fuel Cell Fabrication

The $PrBaMn_2O_{5+\delta}$ (PBMO) powder was prepared with Pechini method. All the nitrate precursors were purchased from Aladdin Co. The powder was calcined at 900°C and then reduced in H_2 for 1 hour to make sure of the existence of oxygen deficiency. $Ce_{0.8}Sm_{0.2}O_{1.9}$ (SDC) were used as electrolyte. The fabrication of the SOFC single cell with the configuration of PBMO anode|PBMO+SDC functional layer/SDC electrolyte/PBMO+SDC functional layer|PBMO cathode was illustrated in Figure 2. Some of the fabrication steps can be found in our previous report. [19] The paste for spin coating is composed of PBMO powder and vehicle paste. The vehicle paste is composed of ethyl cellulose (binder) and terpinol (solvent); the weight ratio of ethyl cellulose to terpinol is 3: 97. The weight ratio of PBMO powder to vehicle paste is 2: 3. And the coating paste can be used after fully mixing in an agate mortar for 1-2 hours. For functional layer, the weight ratio of PBMO to SDC is 7: 3. The slurries were spin coated onto the electrolyte support at 9500 r/min for 1 min. The diameter for the sintered electrolyte supports is 11.3 mm, both electrode diameters are 6.0 mm. The electrochemical performance of the electrodes was tested by an electrochemical workstation (CHI660E, Shanghai Chenhua).

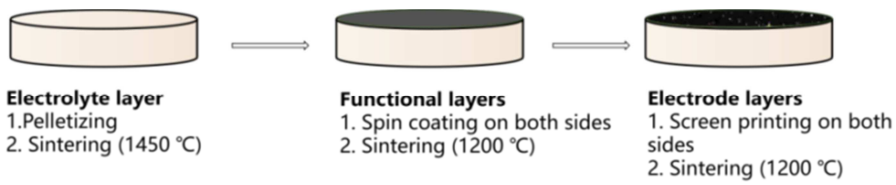

Figure 2. *Schematic diagram of the procedure to fabricate the electrolyte support biogas SOFC.*

For photoanode, the as-prepared MoS_2 nanoflakes on Ti film (MoS_2) and further annealed at 300°C in reducing atmosphere (MoS_2(300°C)) were obtained by a hydrothermal method, and detailed information can be found in our previous

work. [20]

2.3. Material Preparation and Solid Oxide Fuel Cell Fabrication

The phases of materials were analyzed by XRD (with CuK*a* radiation (λ=0.1541 nm). The morphology of the samples were observed by SEM (Hitachi S4800).

The performance of SOFC was tested using simulated biogas (70% CH_4 and 30% CO_2) with 3% water vapor as fuel. The detailed design of test rig is shown in Figure 3. The anode side of the SOFC single cell is sealed by ceramic bond on the top of a quart tube. The transparent quartz tube enables us to insert the alumina fuel inlet tubes, connection of the Pt conducting wires and thermal couples inside of the fuel chamber. The cathode side of the SOFC single cell is exposed to air directly. The output cell current and voltage are detected by an electrochemical workstation (CHI660E, Shanghai Chenhua).

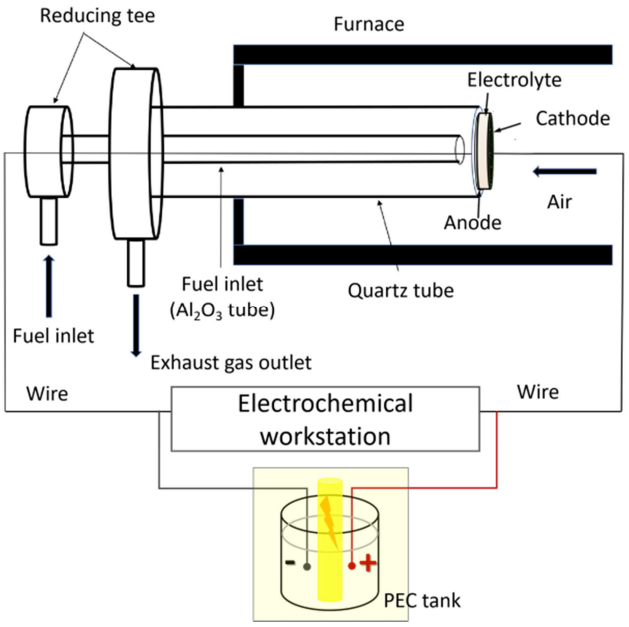

Figure 3. *Schematic diagram of the test rig.*

The PEC degradation of chlorpyrifos (CPF) (10.0 μmol/ L) was carried out with applied bias of 0.5 V in 0.02 M Na_2SO_3 electrolyte, and with pH=3, utilizing an MoS_2 (300°C) electrode (electrode area=1.0 cm^2). Continuous and slow air bubbling into the reactor aimed to provide higher amounts of oxygen for enhancing generation of radicals on the cathode and degradation efficiency. The concentration of CPF at different intervals was analyzed by a gas chromatograph (GC, Fuli 9790). Detailed analytical information can be found in our previous work. [20]

3. Results and Discussion

The SOFC electrode material was characterized by XRD. Figure 4 shows the XRD patterns of originally calcined PBMO, the reduced sample as well as the reduced sample which has been re-calcined in air. The XRD pattern of originally calcined PBMO shows peaks from both tetragonal phase (PDF#97-015-8886) and hexagonal phase (PDF#04-004-7947), as well as some BaO and PrO*x* impurities (PDF#04-006-6521 and PDF#97-015-4588). After it was reduced in H_2 at 900°C for 5 hrs, the peak density of hexagonal phase, BaO and PrO*x* has decreased. This might imply the further reaction of hexagonal phase perovskite, BaO and PrO*x*. Because it will be applied as cathode as well, after re-calcination in air at 900°C for 5 hrs, the powder XRD has been tested again. The peak at the position of 2θ=44.7° might be due to the formation of $BaMnO_{2.88}$ (PDF#97-001-9049). The XRD patterns indicate that both the reduced samples and the re-calcined reduced samples have mainly tetragonal phase and show good chemical and thermal stability because the electrodes work at around 700°C.

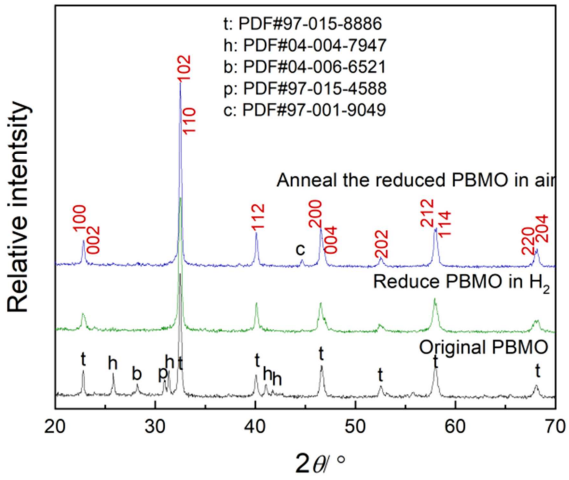

Figure 4. *XRD pattern of originally calcined PBMO sample, reduced sample (in H2 at 900°C for 5 hrs), and the re-calcined reduced sample (in air at 900°C for 5 hrs).*

The Nyquist plots (Figure 5 (a) and (b)) from the impedance test indicate that the R_P values of the PBMO electrodes with PBMO|SDC functional layers were 0.08 and 0.78 Ω·cm^2 in air and simulated biogas respectively, which are acceptable. The Arrhenius plot shown in Figure 5 (c) illustrates the strong temperature dependence of conductivity.

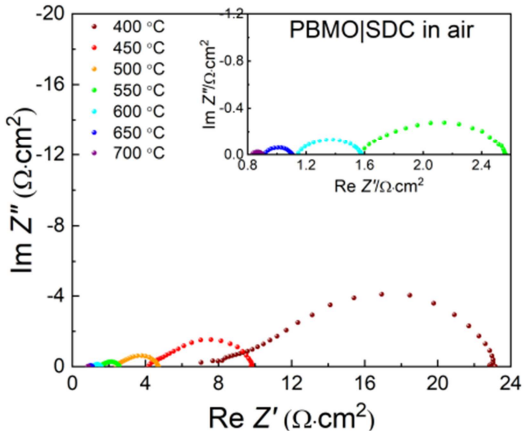

(a)

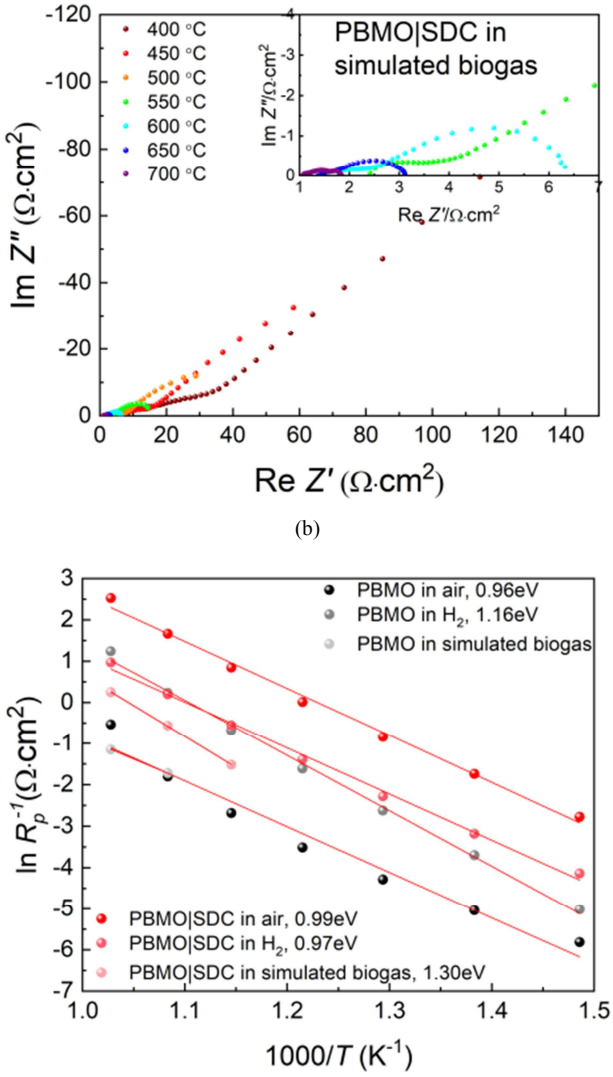

Figure 5. *(a). Nyquist plots of symmetric cell measured at 400-700°C under air. (b). Nyquist plots of symmetric cell measured at 400-700°C under simulated biogas. (c). Arrhenius plots of PBMO electrodes under different working conditions.*

PBMO anode|PBMO+SDC functional layer/SDC electrolyte/PBMO+SDC functional layer|PBMO cathode button cells were fabricated for evaluating the performance of the PBMO electrode based single cell. The inset SEM image in Figure 6. shows the cross section view of the pristine cell. The thickness of SDC electrolyte support is around 100 μm. Both electrode layers attached well with the electrolyte support with enough porosity. Figure 6 (a) depicts the variation of cell voltage and power density as a function of current density using simulated biogas (70% CH_4 and 30% CO_2) with 3% water vapor as the fuel and ambient air as the oxidant in a temperature range of 500−700°C. The maximal power densities of the cell are 325.5 and 234.8 $mW \cdot cm^{-2}$ at 700 and 650°C, respectively. According to Figure 6 (b), with constant biogas input and current density output of 608 $mA \cdot cm^{-2}$, the cell can also have stable voltage output of 0.5 V, which shows the cell stability during operation in biogas.

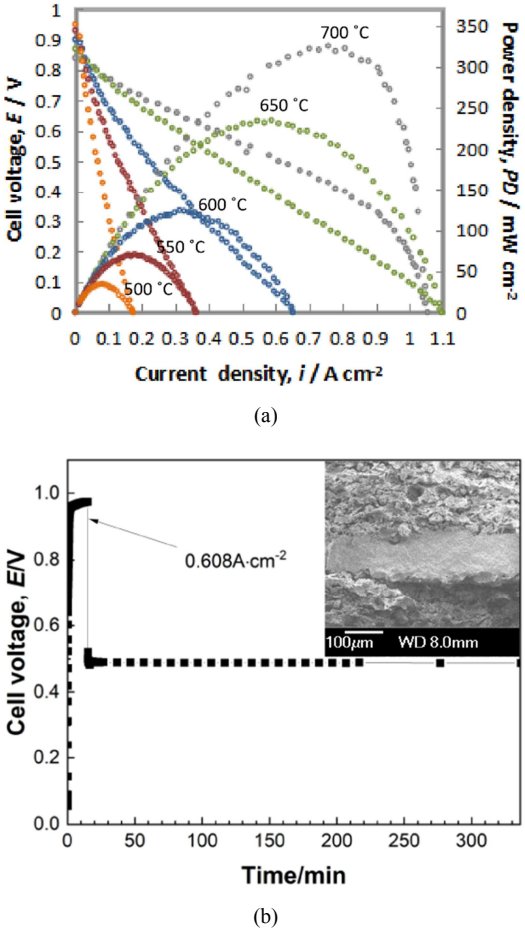

Figure 6. *(a). Variation of cell voltage and power density as a function of current density using simulated biogas (70% CH_4 and 30% CO_2) with 3% water vapor as the fuel and ambient air as the oxidant in a temperature range of 500−700°C; (b). Variation of cell voltage versus time at 700°C with the cell current density stabilized at 0.608 $A \cdot cm^{-2}$. Insert is the SEM image of the cross sectional view of the single cell.*

According to the PEC degradation performance, we can see there is no much difference between the PEC tanks powered by electrochemical workstation and biogas SOFC. The degradation rates of CPF in both PEC tanks can achieve around 99.7%, which indicates that the biogas SOFC can replace the usual power supply to offer voltage bias to the PEC tanks.

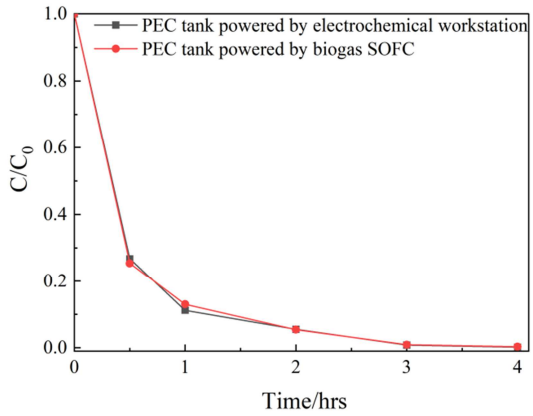

Figure 7. *Degradation rates of chlorpyrifos (CPF) in PEC tanks powered by different power sources versus time.*

The above results in Figure 7 indicate that (1) using simulated biogas (70% CH_4 and 30% CO_2) with 3% water vapor as the fuel and ambient air as the oxidant, the power density of PBMO-based SOFC can achieve 325.5 and 234.8 $mW \cdot cm^{-2}$ at 700 and 650°C, respectively. And with constant current density input of 608 $mA \cdot cm^{-2}$, the biogas SOFC can also have stable voltage output of 0.5 V. This shows the stability of the biogas SOFC.

With applied bias of 0.5 V in 0.02 M Na_2SO_3 electrolyte, and with pH=3, the degradation rate of chlorpyrifos (CPF) by PEC tank can achieve 99.7% after 4 hours, which is comparable with the degradation rate (99.7%) in the PEC tank powered by the electrochemical workstation. This means the PEC tanks paired with biogas SOFC can degrade CPF well.

4. Conclusion

In this research, the $PrBaMn_2O_{5+\delta}$ (PBMO) powder was prepared via Pechini method. The as-prepared $PrBaMn_2O_{5+\delta}$ electrodes show good chemical and thermal stability in both reduced and oxidized atmosphere. The R_P values of the PBMO electrodes with PBMO|SDC functional layers were 0.08 and 0.78 $\Omega \cdot cm^2$ in air and simulated biogas respectively, which are acceptable. Using PBMO as electrodes, with constant biogas input and current density output of 608 $mA \cdot cm^{-2}$, the biogas SOFC can have stable voltage output of 0.5 V, which shows the cell stability during operation in biogas. With MoS_2 nanoflakes on Ti film as photoanode, the PEC tank can be connected and paired with the biogas SOFC.

According to the preliminary experiment results in this report, this SOFC-PEC paired system shows the potential to reduce the total energy consumption and to lower the greenhouse gas emission in traditional wastewater treatment facilities, by effectively utilizing the biogas discharged during sewage treatment or garbage landfill processes. But due to the long term stability of SOFC still needs improvement, this might be the pivotal hindrance for the large scale application of SOFC-PEC paired system.

Acknowledgments

The authors are grateful for the financial support from Basic research program of Guangdong Province (No. 2018A030313851), Shenzhen Science and Technology Innovation Commission (Grant No. JCYJ20190813171403664) and Longgang District Technology Supporting Project (No. LGKCKJPT2019074).

References

[1] Q. Wang, X. Li, W. Liu, et al., "Carbon source recovery from waste sludge reduces greenhouse gas emissions in a pilot-scale industrial wastewater treatment plant," Environmental Science and Ecotechnology, vol. 14, 2022, pp. 100235-100242.

[2] H. Wang, Y. Yang, A. A. Keller, et al., "Comparative analysis of energy intensity and carbon emissions in wastewater treatment in USA, Germany, China and South Africa," Applied Energy, vol. 184 2016, pp. 873-881.

[3] Z. Hao, R. Wang, L. Zhang, et al., "More comprehensive heterojunction mechanism: Enhanced PEC properties originated from novel $ZnIn_2S_4/Cu_2S$ heterojunction assisted by changed surface states," Chemical Engineering Journal, vol. 468, 2023, pp. 143568-143578.

[4] C. Liu, D. Kong, P. C. Hsu, et al., "Rapid water disinfection using vertically aligned MoS_2 nanofilms and visible light," Nature Nanotechnology, vol. 11, 2016, pp. 1098-1104.

[5] B. Illathukandy, S. A. Saadabadi, P-C Kuo, et al., "Solid oxide fuel cells (SOFCs) fed with biogas containing hydrogen chloride traces: Impact on direct internal reforming and electrochemical performance," Electrochimica Acta, vol. 433, 2022, pp. 141198-141210.

[6] J. Yan, Z. G. Chen, H. Y. Ji, et al., "Cover Picture: Construction of a 2D graphene-like MoS_2/C_3N_4 heterojunction with enhanced visible-light photocatalytic activity and photoelectrochemical activity," Chemistry-A European Journal, vol. 22, 2016, pp. 4764-4773.

[7] S. W. Tao, J. T. S. Irvine, "Synthesis and characterization of $(La_{0.75}Sr_{0.25})Cr_{0.5}Mn_{0.5}O_{3-\delta}$, a redox-stable, efficient perovskite anode for SOFCs," J. Electrochem. Soc., vol. 151, 2004, pp. A252-259.

[8] R. Mukundan, E. L. Brosha, F. H. Garzon, "Sulfur tolerant anodes for SOFCs," Electrochem Solid-State Lett., vol. 7, 2004, pp. A5-A7.

[9] Q. X. Fu, F. Tietz, D. St¨over, "$La_{0.4}Sr_{0.6}Ti_{1-x}Mn_xO_{3-\delta}$ perovskites as anode materials for solid oxide fuel cells," J. Electrochem. Soc., vol. 153, 2006, pp. D74-D83.

[10] X. Sun, S. Wang, Z. Wang, X. Ye, T. Wen, F. Huang, "Anode performance of LST–xCeO$_2$ for solid oxide fuel cells," J. Power Sources, vol. 183, 2008, pp. 114-117.

[11] J. C. Ruiz-Morales, J. Canales-Vázquez, C. Savaniu, D. Marrero-López, W. Zhou and J. T. S. Irvine, "Disruption of extended defects in solid oxide fuel cell anode for methane oxidation," Nature, vol. 439, 2006, pp. 568-571.

[12] X. J. Chen, Q. L. Liu, S. H. Chan, N. P. Brandon, K. A. Khor, "High performance cathode-supported SOFC with perovskite anode operating in weakly humidified hydrogen and methane," Electrochem. Commun., vol. 9, 2007, pp. 767-772.

[13] Y. H. Huang, R. I. Dass, Z. L. Xing, J. B. Goodenough, "Double perovskites as anode materials for solid oxide fuel cells," Science, vol. 31, 2006, pp. 254-257.

[14] Q. Zhang, T. Wei, Y.-H. Huang, "Electrochemical performance of double-perovskite Ba_2MMoO_6 (M = Fe, Co, Mn, Ni) anode materials for solid oxide fuel cells," J. Power Sources, vol. 198, 2012, pp. 59-65.

[15] L. Yang, S. Wang, K. Blinn, M. Liu, Z. Liu, Z. Cheng, M. Liu, "Enhanced sulfur and coking tolerance of a mxed ion conductor for SOFCs: $BaZr_{0.1}Ce_{0.7}Y_{0.2-x}Yb_xO_{3-\delta}$," Science, vol. 326, 2009, pp. 126-129.

[16] S. Sengodan, S. Choi, A. Jun, T. H. Shin, Y.-W. Ju, H. Y. Jeong, J. Shin, J. T. S. Irvine, G. Kim, "Layered Oxygen-Deficient Double Perovskite as an Efficient and Stable Anode for Direct Hydrocarbon Solid Oxide Fuel Cells," Nat. Mater., vol. 14, 2014, pp. 205–209.

[17] S. Choi, S. Sengodan, S. Park, Y. W. Ju, J. Kim, J. Hyodo, H. Y. Jeong, T. Ishihara, J. Shin, G. Kim, "A robust symmetrical electrode with layered perovskite structure for direct hydrocarbon solid oxide fuel cells: $PrBa_{0.8}Ca_{0.2}Mn_2O_{5+\delta}$. J. Mater. Chem. A, vol. 4, 2016, pp. 1747−1753.

[18] Y.-F. Sun, Y.-Q. Zhang, B. Hua, Y. Behnamian, J. Li, S.-H. Cui, J.-H. Li, J.-L. Luo, "Molybdenum doped $Pr_{0.5}Ba_{0.5}MnO_{3-\delta}$ (Mo-PBMO) double perovskite as a potential solid oxide fuel cell anode material," J. Power Sources, vol. 301, 2016, pp. 237-241.

[19] D. Gu, G. Zhang, J. Zou., "High temperature thermo-photocatalysis driven carbon removal in direct biogas fueled solid oxide fuel cells," Chinese Chemical Letters, vol. 32, 2021, pp. 3548-3552.

[20] Y. Zhou, G. Zhang, J. Zou, "Photoelectrocatalytic generation of miscellaneous oxygen-based radicals towards cooperative degradation of multiple organic pollutants in water," Water Reuse, vol. 11, 2021, pp. 531-541.